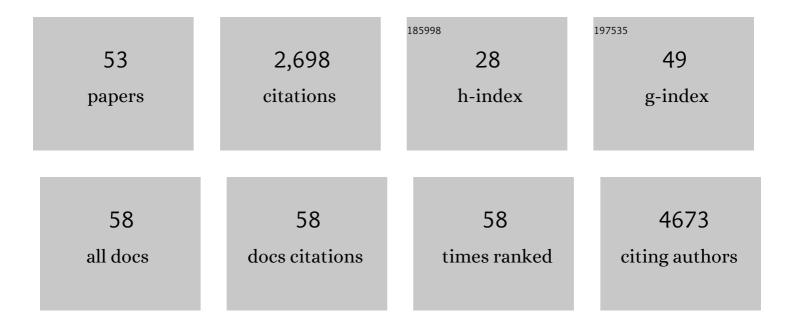
## Karl Harlos

List of Publications by Year in descending order

Source: https://exaly.com/author-pdf/5872884/publications.pdf Version: 2024-02-01



#	Article	IF	CITATIONS
1	Initiation of T cell signaling by CD45 segregation at 'close contacts'. Nature Immunology, 2016, 17, 574-582.	7.0	253
2	A procedure for setting up high-throughput nanolitre crystallization experiments. Crystallization workflow for initial screening, automated storage, imaging and optimization. Acta Crystallographica Section D: Biological Crystallography, 2005, 61, 651-657.	2.5	234
3	Toremifene interacts with and destabilizes the Ebola virus glycoprotein. Nature, 2016, 535, 169-172.	13.7	210
4	The ligand-binding face of the semaphorins revealed by the high-resolution crystal structure of SEMA4D. Nature Structural and Molecular Biology, 2003, 10, 843-848.	3.6	143
5	Structure of a Pestivirus Envelope Glycoprotein E2 Clarifies Its Role in Cell Entry. Cell Reports, 2013, 3, 30-35.	2.9	124
6	FLRT Structure: Balancing Repulsion and Cell Adhesion in Cortical and Vascular Development. Neuron, 2014, 84, 370-385.	3.8	117
7	High-speed fixed-target serial virus crystallography. Nature Methods, 2017, 14, 805-810.	9.0	106
8	Structure and functional properties of Norrin mimic Wnt for signalling with Frizzled4, Lrp5/6, and proteoglycan. ELife, 2015, 4, .	2.8	90
9	Structure of a phleboviral envelope glycoprotein reveals a consolidated model of membrane fusion. Proceedings of the National Academy of Sciences of the United States of America, 2016, 113, 7154-7159.	3.3	87
10	Crystal Structure of the Herpesvirus Nuclear Egress Complex Provides Insights into Inner Nuclear Membrane Remodeling. Cell Reports, 2015, 13, 2645-2652.	2.9	80
11	The crystal structure of human dopamine β-hydroxylase at 2.9 à resolution. Science Advances, 2016, 2, e1500980.	4.7	80
12	Shielding and activation of a viral membrane fusion protein. Nature Communications, 2018, 9, 349.	5.8	78
13	Unexpected structure for the N-terminal domain of hepatitis C virus envelope glycoprotein E1. Nature Communications, 2014, 5, 4874.	5.8	72
14	Targeting Prolyl-tRNA Synthetase to Accelerate Drug Discovery against Malaria, Leishmaniasis, Toxoplasmosis, Cryptosporidiosis, and Coccidiosis. Structure, 2017, 25, 1495-1505.e6.	1.6	68
15	A Molecular-Level Account of the Antigenic Hantaviral Surface. Cell Reports, 2016, 15, 959-967.	2.9	57
16	Pathogen-derived HLA-E bound epitopes reveal broad primary anchor pocket tolerability and conformationally malleable peptide binding. Nature Communications, 2018, 9, 3137.	5.8	57
17	Structural basis for the activity of a cytoplasmic RNA terminal uridylyl transferase. Nature Structural and Molecular Biology, 2012, 19, 782-787.	3.6	47
18	Structure and Self-Assembly of the Calcium Binding Matrix Protein of Human Metapneumovirus. Structure, 2014, 22, 136-148.	1.6	44

KARL HARLOS

#	Article	IF	CITATIONS
19	Structural Insights into the Inhibition of Wnt Signaling by Cancer Antigen 5T4/Wnt-Activated Inhibitory Factor 1. Structure, 2014, 22, 612-620.	1.6	42
20	Crystal Structure of Insulin-Regulated Aminopeptidase with Bound Substrate Analogue Provides Insight on Antigenic Epitope Precursor Recognition and Processing. Journal of Immunology, 2015, 195, 2842-2851.	0.4	41
21	A Protective Monoclonal Antibody Targets a Site of Vulnerability on the Surface of Rift Valley Fever Virus. Cell Reports, 2018, 25, 3750-3758.e4.	2.9	41
22	Specific Stereoisomeric Conformations Determine the Drug Potency of Cladosporin Scaffold against Malarial Parasite. Journal of Medicinal Chemistry, 2018, 61, 5664-5678.	2.9	41
23	Structure of glycosylated <scp>NPC</scp> 1 luminal domain C reveals insights into <scp>NPC</scp> 2 and Ebola virus interactions. FEBS Letters, 2016, 590, 605-612.	1.3	39
24	Drastic changes in conformational dynamics of the antiterminator M2-1 regulate transcription efficiency in Pneumovirinae. ELife, 2014, 3, e02674.	2.8	39
25	Structural Transitions of the Conserved and Metastable Hantaviral Glycoprotein Envelope. Journal of Virology, 2017, 91, .	1.5	38
26	The structure of a prokaryotic viral envelope protein expands the landscape of membrane fusion proteins. Nature Communications, 2019, 10, 846.	5.8	37
27	Pushing the limits of sulfur SAD phasing: <i>de novo</i> structure solution of the N-terminal domain of the ectodomain of HCV E1. Acta Crystallographica Section D: Biological Crystallography, 2014, 70, 2197-2203.	2.5	33
28	Ligand-Induced Conformational Change of Insulin-Regulated Aminopeptidase: Insights on Catalytic Mechanism and Active Site Plasticity. Journal of Medicinal Chemistry, 2017, 60, 2963-2972.	2.9	33
29	Structures of monomeric and oligomeric forms of the <i>Toxoplasma gondii</i> perforin-like protein 1. Science Advances, 2018, 4, eaaq0762.	4.7	32
30	Convergent immunological solutions to Argentine hemorrhagic fever virus neutralization. Proceedings of the National Academy of Sciences of the United States of America, 2017, 114, 7031-7036.	3.3	31
31	Structure of astrotactin-2: a conserved vertebrate-specific and perforin-like membrane protein involved in neuronal development. Open Biology, 2016, 6, 160053.	1.5	28
32	Structural plasticity of Cid1 provides a basis for its distributive RNA terminal uridylyl transferase activity. Nucleic Acids Research, 2015, 43, 2968-2979.	6.5	25
33	New insights into the enzymatic mechanism of human chitotriosidase (CHIT1) catalytic domain by atomic resolution X-ray diffraction and hybrid QM/MM. Acta Crystallographica Section D: Biological Crystallography, 2015, 71, 1455-1470.	2.5	23
34	A key region of molecular specificity orchestrates unique ephrin-B1 utilization by Cedar virus. Life Science Alliance, 2020, 3, e201900578.	1.3	22
35	Four crystal structures of human LLT1, a ligand of human NKR-P1, in varied glycosylation and oligomerization states. Acta Crystallographica Section D: Biological Crystallography, 2015, 71, 578-591.	2.5	20
36	Structural basis of malaria parasite phenylalanine tRNA-synthetase inhibition by bicyclic azetidines. Nature Communications, 2021, 12, 343.	5.8	19

KARL HARLOS

#	Article	IF	CITATIONS
37	Structure of 6-hydroxymethyl-7,8-dihydropterin pyrophosphokinase–dihydropteroate synthase from Plasmodium vivax sheds light on drug resistance. Journal of Biological Chemistry, 2018, 293, 14962-14972.	1.6	18
38	Structural basis of semaphorinâ€plexin <i>cis</i> interaction. EMBO Journal, 2020, 39, e102926.	3.5	17
39	Mouse and human antibodies bind HLA-E-leader peptide complexes and enhance NK cell cytotoxicity. Communications Biology, 2022, 5, 271.	2.0	14
40	Structure of the Wnt signaling enhancer <scp>LYPD</scp> 6 and its interactions with the Wnt coreceptor <scp>LRP</scp> 6. FEBS Letters, 2018, 592, 3152-3162.	1.3	13
41	Natural Killer Cell Activation Receptor NKp30 Oligomerization Depends on Its N-Glycosylation. Cancers, 2020, 12, 1998.	1.7	12
42	Disruption of the dimerization interface of the sensing domain in the dimeric heme-based oxygen sensor AfGcHK abolishes bacterial signal transduction. Journal of Biological Chemistry, 2020, 295, 1587-1597.	1.6	11
43	A Twoâ€Tailed Phosphopeptide Crystallizes to Form a Lamellar Structure. Angewandte Chemie - International Edition, 2017, 56, 3252-3255.	7.2	10
44	Diversity of oligomerization in Drosophila semaphorins suggests a mechanism of functional fine-tuning. Nature Communications, 2019, 10, 3691.	5.8	10
45	Structure of the Human Cation-Independent Mannose 6-Phosphate/IGF2 Receptor Domains 7–11ÂUncovers the Mannose 6-Phosphate Binding Site of Domain 9. Structure, 2020, 28, 1300-1312.e5.	1.6	8
46	Crystal structures of the two domains that constitute the <i>Plasmodium vivax</i> p43 protein. Acta Crystallographica Section D: Structural Biology, 2020, 76, 135-146.	1.1	8
47	Inhibition of Plasmodium falciparum Lysylâ€ŧRNA Synthetase via a Piperidineâ€Ring Scaffold Inspired Cladosporin Analogues. ChemBioChem, 2021, 22, 2468-2477.	1.3	7
48	Contrasting Modes of New World Arenavirus Neutralization by Immunization-Elicited Monoclonal Antibodies. MBio, 2022, 13, e0265021.	1.8	7
49	Insights from the crystal structure of the chicken CREB3 bZIP suggest that members of the CREB3 subfamily transcription factors may be activated in response to oxidative stress. Protein Science, 2019, 28, 779-787.	3.1	5
50	Inhibition of Plasmodium falciparum phenylalanine tRNA synthetase provides opportunity for antimalarial drug development. Structure, 2022, 30, 962-972.e3.	1.6	4
51	Structural Analysis and Development of Notum Fragment Screening Hits. ACS Chemical Neuroscience, 2022, 13, 2060-2077.	1.7	3
52	Improved crystallization and diffraction of caffeine-induced death suppressor protein 1 (Cid1). Acta Crystallographica Section F, Structural Biology Communications, 2015, 71, 346-353.	0.4	2
53	A Twoâ€Tailed Phosphopeptide Crystallizes to Form a Lamellar Structure. Angewandte Chemie, 2017, 129, 3300-3303.	1.6	Ο